energies

MDPI

Article

# The Use of Dolomite to Produce a Magnesium Potassium Phosphate Matrix for Radioactive Waste Conditioning

**Svetlana A. Kulikova *, Kseniya Y. Belova, Anna V. Frolova and Sergey E. Vinokurov ***

Vernadsky Institute of Geochemistry and Analytical Chemistry, Russian Academy of Sciences, 19 Kosygin St., 119991 Moscow, Russia; ksysha_3350@mail.ru (K.Y.B.); annav1805@gmail.com (A.V.F.)

* Correspondence: kulikova.sveta92@mail.ru (S.A.K.); vinokurov.geokhi@gmail.com (S.E.V.); Tel.: +7-495-939-7007 (S.A.K.)

**Abstract:** Magnesium potassium phosphate (MPP) matrix $MgKPO_4 \times 6H_2O$ is a known material for radioactive waste (RW) conditioning; magnesium oxide MgO is used in the classical method of matrix synthesis. The aim of the work was to investigate the possibility of using the widely available natural mineral raw material dolomite, incorporating mixed magnesium and calcium carbonate, for the production of this matrix. To control the quality of the samples obtained, their phase and elemental compositions, microstructure, density, volumetric and apparent porosity, compressive strength, and hydrolytic stability were studied. As a result, it was found that using dolomite powder pre-calcined at 720 °C for 1.5 h, samples of matrix whose properties meet the regulatory requirements for solidified RW were obtained. Thus, a new, cost-effective method of synthesis of the MPP matrix has been demonstrated to solve the RW solidification problem.

**Keywords:** magnesium potassium phosphate matrix; radioactive waste; dolomite; compressive strength; hydrolytic stability; particle size distribution; specific surface area; structure; porosity

check for updates

**Citation:** Kulikova, S.A.; Belova, K.Y.; Frolova, A.V.; Vinokurov, S.E. The Use of Dolomite to Produce a Magnesium Potassium Phosphate Matrix for Radioactive Waste Conditioning. *Energies* **2023**, *16*, 5513. https://doi.org/10.3390/en16145513

Academic Editor: Jong-Il Yun

Received: 15 June 2023
Revised: 8 July 2023
Accepted: 19 July 2023
Published: 20 July 2023



## 1. Introduction

Radioactive waste (RW) is generated during activities using radioisotopes in the nuclear industry, science, and medicine, as well as during the operation and decommissioning of nuclear facilities. Such waste must be handled in a way that ensures the radiation safety of people and the environment for long periods of time [1]. At the same time, the generated RW must be conditioned using stable preservation matrices for their subsequent safe storage or final disposal [2,3].

Glass is the only industrial matrix for conditioning high-level waste (HLW) used in Russia, UK, the USA, France, Germany, Belgium, China, Japan, and other countries [2,4].

However, vitrification of waste has a number of disadvantages due to the high energy intensity, high cost, and massive amount of high-temperature vitrification equipment with a short technical lifetime, which, after termination of operation, becomes "secondary" RW, the management of which is currently an unresolved problem.

Cement is the matrix for conditioning intermediate-level waste (ILW) that has been practiced for many years in a number of countries [5]. At the same time, in a recent review [6], it was noted that further research in the development of mineral matrices based on alternative cement-like materials for conditioning various RW types would contribute to the further sustainable development of RW management systems. Alternative binders have expanded the possibilities and prospects for cementation of toxic materials [6] and metal wastes containing uranium [7] and aluminum [8], which are incompatible with Portland cement due to its high alkalinity and high free water content in conventional systems [9]. The main advantage of cement-like materials is their low-temperature (<100 °C) synthesis without high capital costs [10].

One possible alternative to these matrices is chemically bonded phosphate ceramics [11], which include a mineral-like magnesium potassium phosphate (MPP) matrix. Earlier, we

showed in [4,12,13] that MPP matrix of the composition $MgKPO_4 \times 6H_2O$ is an effective and multipurpose material for conditioning of RW, including ILW and HLW. The MPP matrix is produced at room temperature by reaction (1) and is an analogue of the natural mineral struvite-K [14]. Crystal structure of struvite-K is given in [6,14].

$$MgO + KH_2PO_4 + 5H_2O \rightarrow MgKPO_4 \times 6H_2O \quad (1)$$

The advantage of MPP matrix in comparison with Portland cement is higher efficiency of both physical and chemical immobilization of heavy metals and radionuclides [6,15–17]. Chemical immobilization of waste components is provided due to ion-exchange properties of K-struvite in the structure of which substitution of potassium and magnesium for other univalent cations ($NH^{4+}$, $K^+$, $Rb^+$, $Cs^+$, $Tl^+$) and divalent cations ($Mg^{2+}$, $Ni^{2+}$, $Zn^{2+}$, $Co^{2+}$, $Cd^{2+}$, $Cr^{3+}$, $Mn^{2+}$, $VO^{2+}$) respectively is possible [6,18–20]. At the same time the MPP matrix has high radiation resistance to gamma and alpha irradiation [21], including electron irradiation up to $10^8$ Gy [4].

MgO is the hardener in reaction (1). At the same time, when using commercial MgO samples, a number of conditions should be taken into account, primarily the optimal characteristics of MgO powder to obtain an MPP matrix [22]. It is known that the use of MgO requires pre-calcination at a high temperature (usually 1300 °C) to reduce its dissolution rate and increase the setting time of the mixture in reaction (1), which increases the cost of raw materials [23]. The cost of individual commercial samples of MgO can reach thousands of dollars or more per ton, which exceeds the cost of Portland cement [24,25].

At the same time, the minerals magnesite and dolomite (base-magnesium and magnesium -calcium carbonates, respectively) are known to be used as sources of magnesium [25]. MgO is obtained by calcination of these carbonate minerals at a high temperature of 1300–1500 °C [11,20,25–27]. In addition, the magnesite reserves are geographically limited to certain countries (e.g., China—27%, North Korea—24%, Russia—22%) [27]. At the same time, dolomite is the most common high-magnesia rock; its reserves are huge, and if we consider that a significant part of dolomite and dolomitized magnesite has already been mined and is now in dumps, it makes dolomitized rocks a promising raw material for the production of binders [20].

It is known that thermal decarbonization of dolomite occurs in two stages [20,27–30]. First, MgO and calcite ($CaCO_3$) are formed by the reaction (2) at temperatures starting at 670 °C [20,30]. At the same time, when the temperature rises to ~750 °C, calcite decomposes to calcium oxide (CaO) according to the reaction (3) [27]. It was noted in [29] that the simultaneous formation of calcite, lime, and periclase in air, accompanied by the decomposition of dolomite, was observed at temperatures between 700 and 750 °C. It is noted [20] that these reactions often proceed in a single stage in air. In addition, it is noted that there may be different decomposition temperatures for dolomite depending on its purity and conditions of decomposition [20].

$$(Mg,Ca)(CO_3)_2 \rightarrow MgO + CaCO_3 + CO_2 \quad (2)$$

$$CaCO_3 \rightarrow CaO + CO_2 \quad (3)$$

In the study [25], it was noted that dolomite fired at high temperatures always contains CaO, so it cannot be used directly to obtain MPP matrix as a magnesia raw material—hardener in the reaction (1). The presence of CaO can lead to a faster setting of the mixture, because CaO has a higher reactivity than MgO [27].

At the same time, we have previously shown the possibility of including up to 50 wt% $CaCO_3$ into the MPP matrix in order to use it for conditioning RW containing $^{14}C$ and established its high-quality parameters (compressive strength, hydrolytic stability, etc.) and minimal carryover of $CO_2$ into the atmosphere during synthesis and exposure of compounds [31]. Thus, dolomite powder, calcined in accordance with the reaction (2) and thus containing MgO and $CaCO_3$, is considered a promising raw material that serves as a source of magnesium.

In the present study, a new method of synthesis of MPP matrix using dolomite as a cheap source of MgO is considered. In addition, the effect of the calcination temperature of dolomite on its composition and the properties of the resulting matrix was studied.

## 2. Materials and Methods

### *2.1. Characteristics of Used Dolomite Powder*

A commercial powder sample LR-55 (LLC "Laurens", Novosibirsk, Russia) obtained from the natural mineral dolomite of the Taenzinsky deposit (Kemerovo region, Russia) was used as a magnesia material. The particle size of the initial sample was <0.16 mm.

Adsorption measurements of dolomite samples were performed on an ASAP 2000 automatic sorbtometer (Micromeritics, Norcross, GA, USA). The specific surface area of the dolomite samples was determined with the software package Micromeritics. Samples were pretreated at 120 °C under vacuum. The specific surface area of the initial dolomite powder was about 12.2 $m^2/g$.

The elemental composition of dolomite samples was preliminarily studied by the X-ray fluorescence (XRF) method using an Axious Advanced PW 4400/04 spectrometer (PANalytical B.V., Almelo, The Netherlands). The loss on ignition (LOI) at 950 °C was determined. Its chemical composition in oxide wt% was: MgO—26.68; CaO—36.30; $SiO_2$—0.44; $Al_2O_3$—0.28; impurities of other elements—no more than 0.30, loss on ignition—36.17 (Table 1).

**Table 1.** Chemical composition of initial samples of dolomite according to XRF data.

| Chemical Compound | Composition (wt%) |
|---|---|
| MgO | 26.68 |
| CaO | 36.30 |
| $SiO_2$ | 0.44 |
| $Al_2O_3$ | 0.28 |
| $TiO_2$ | 0.014 |
| $Fe_2O_3$ | 0.14 |
| $K_2O$ | 0.01 |
| $P_2O_5$ | 0.10 |
| Cr | 0.0015 |
| Cu | 0.0027 |
| Zn | 0.0040 |
| Rb | 0.0008 |
| Sr | 0.0102 |
| Y | 0.0006 |
| Zr | 0.0016 |
| Nb | 0.0008 |
| Pb | 0.0101 |
| LOI * | 36.17 |

* LOI—Loss on ignition: stable weight loss was achieved at 950 °C.

The sample's microstructure was analyzed by scanning electron microscopy (SEM) using a Mira3 microscope (Tescan, Brno, Czech Republic). Electron probe microanalysis of the samples of dolomite and MPP matrix was carried out by energy-dispersive X-ray spectroscopy (EDS) on an X-Max analyzer (Oxford Inst., High Wycombe, UK). The results of SEM/EDS analysis are shown in Figure S1a and Table S1 (see Supplementary Materials).

The calcination temperature of the experimental sample of dolomite was chosen based on known data (Section 1) and preliminary experiments on its decomposition as a function of temperature and calcination time. So, dolomite was calcined to obtain MgO and $CaCO_3$ according to the reaction (2) at 720 °C for 1.5 h (heating rate was 4 °C/min, cooling was natural) in a SNOL 30/1300 muffle furnace (AB UMEGA GROUP, Utena, Lithuania).

For comparison, we also prepared a sample calcined at 750 °C for 28 h according to the reactions (2) and (3) to obtain MgO and CaO from the decomposition of $CaCO_3$.

### 2.2. Synthesis of the MPP Matrix Samples

The MPP matrix samples were synthesized by reaction (1) at a weight ratio of $MgO:H_2O:KH_2PO_4$ of 1:2:3. The mass of calcined dolomite powders used was calculated taking into account the MgO content. Potassium dihydrogen phosphate ($KH_2PO_4$, GOST 4198-15, "Rushim" LLC, Moscow, Russia) with a particle size of 0.15–0.25 mm was used to produce MPP matrix. Boric acid ($H_3BO_3$, GOST 9656-75, "JSC REAHIM" LLC, Moscow, Russia) was used as a retardant of the reaction (1) in an amount of about 1.5 wt% of the sample mass.

In the text below, the designation of the obtained matrix samples is as follows: MPP_dolomite_720 and MPP_dolomite_750 were obtained using dolomite calcined at 720 and 750 °C, respectively.

Cesium nitrate ($CsNO_3$, TU 6-09-437-83, Lenreaktiv, Saint Petersburg, Russia) and lanthanum nitrate ($La(NO_3)_3 \times 6H_2O$, TU 2323-004-29923808-2016, "LenReaktiv" JSC, Saint Petersburg, Russia) were used as fission product simulators from the RW composition. The content of Cs and La was 4 wt% in the samples.

The cubic 2 × 2 × 2 cm samples of the MPP matrix were obtained. Samples were stored under ambient atmospheric conditions for at least 14 days before studying their properties.

### 2.3. Research Methods for Experimental Samples

The particle size distribution of the dolomite powder samples was measured with an Analysette 22 NanoTec laser diffraction granulometer (Fritsch, Idar-Oberstein, Germany). The sizes of the studied particles varied from 0.01 to 1000 μm. The size distribution was determined by an algorithm using the integral Fredholm equation.

The phase composition of samples of dolomite and MPP matrix was determined using an MiniFlex 600 X-ray diffractometer (Rigaku, Tokyo, Japan) by X-ray diffraction (XRD). XRD data was analyzed using the Rigaku SmartLab Studio II software (Ver.4.5.286.0) with the PDF-2 database. The composition of dolomite was determined using the Rietveld method.

The density ($\rho_v$, g/cm$^3$) of MPP matrix samples were determined by hydrostatic weighing based on the Archimedes principle by the Equation (4). The volumetric (PV) and apparent porosity (PA) of the MPP matrix samples was determined by Equations (5) and (6), respectively. The samples were weighed while they were still dry ($M_{dry}$). Furthermore, the samples were immersed in water, and their mass was determined at the initial moment ($M_i$), after which they were left immersed in water for 24 h until they became fully saturated. The mass of the immersion ($M_{i,24h}$) and the mass of the wet sample ($M_{wet}$) were then determined.

$$\rho_v = \frac{m}{V} = \frac{M_{dry}}{(M_{dry} - M_{i,24})} \quad (4)$$

$$PV = \frac{V_{pores}}{V_{sample}} = \frac{(M_{i,24h} - M_i)}{(M_{dry} - M_{i,24h})} \cdot 100 \quad (5)$$

$$PA = \frac{(M_{wet} - M_{dry})}{(M_{wet} - M_{i,24h})} \cdot 100 \quad (6)$$

The compressive strength of cubic samples of the MPP matrix was measured with a Cybertronic 500/50 kN testing machine (Testing Bluhm & Feuerherdt GmbH, Berlin, Germany).

Hydrolytic stability of the MPP matrix samples was evaluated at 25 ± 3 °C in accordance with the Russian standard test GOST R 52126-2003 [32]. Before leaching, monolithic samples were immersed in ethanol for 5–7 s to clean them from mechanical impurities. Washed samples were air-dried for 30 min. Furthermore, cubic samples with an area of open geometric surface were immersed in a PTFE container with a solution of a leaching agent. The leaching agent was double-distilled water (pH 6.6 ± 0.1, volume 100 cm$^3$), which was replaced at regular time intervals. Samples were removed from the container at the set time, washed with double-distilled water (volume 100 cm$^3$), and mixed with the

leachate. The content of the matrix components in the solutions after leaching of MPP matrix was determined by the ICP-AES method (iCAP-6500 Duo, Thermo Scientific, Waltham, MA, USA). The content of cesium and lanthanum in the solutions was determined by the ICP-MS method (X Series2, Thermo Scientific, Waltham, MA, USA). The experimental and instrumental errors did not exceed the relative values of 30% due to the low contents of elements in solutions after leaching.

The differential leaching rate (LR) [g/(cm$^2$·day)] of compound components from the samples was calculated according to Equation (7).

$$LR = \frac{c \cdot V}{S \cdot f \cdot t}, \quad (7)$$

where c—concentration of element in the solution, g/L; V—volume of double distilled water, L; S—area of open geometric surface of sample, cm$^2$; f—content of element in matrix, g/g; t—duration of the *n*-th leaching period, days.

## 3. Results and Discussion

### *3.1. Effect of Calcination of Dolomite*

The obtained data on the granulometric composition of dolomite powder samples are presented in Figure 1. The particle size distribution of the used samples of calcined powders of dolomite can be characterized as polymodal. At the same time, it can be seen from Figure 1 that the sample calcined at 720 °C consists of particles with a size of no more than 45 µm. It should be noted that in the study [33], it was observed that heat treatment below 727 °C has a small effect on the particle size distribution.

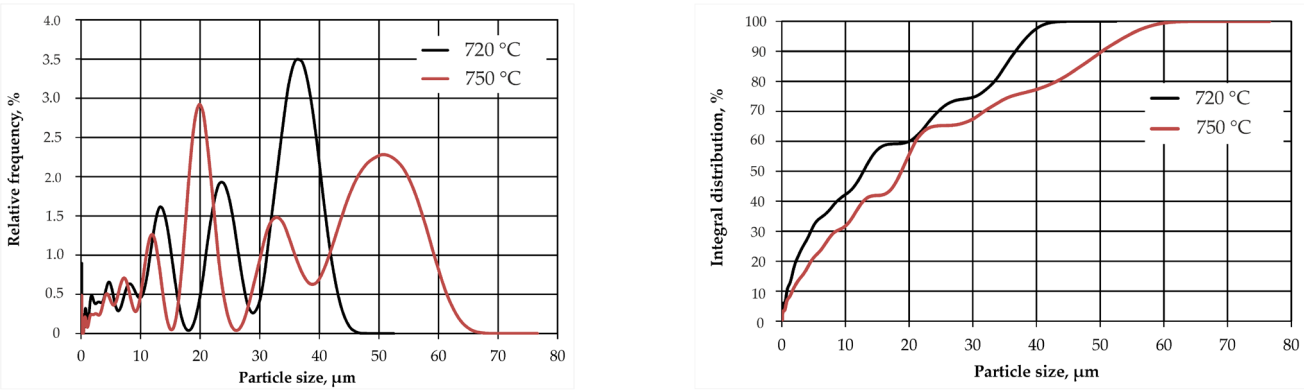


(**a**) (**b**)

**Figure 1.** Size distribution of dolomite powder samples calcined at 720 °C and 750 °C. (**a**) relative frequency; (**b**) integral distribution.

An increase in particle size and partial agglomeration occurs when dolomite is calcined at 750 °C (Figure 1). It was shown that about 20% of the particles acquire a size in the range of 45–65 µm (Figure 1b).

On the other hand, increasing the calcination temperature from 720 °C to 750 °C does not affect the specific surface area, which is about 3.6 m$^2$/g.

The initial dolomite sample (Figure 2a) consisted of phases of calcite ($CaCO_3$, main reflexes at 3.04, 2.28, 2.09 Å etc.), periclase (MgO, main reflexes at 2.11, 1.49 Å etc.), and dolomite ($CaMg(CO_3)_2$, main reflexes at 2.88, 2.19, 1.79 Å etc.), which was confirmed by the XRD method. When this sample is calcined at 720 °C (Figure 2b), magnesium carbonate decomposes to magnesium oxide, and calcium carbonate partially decomposes to calcium oxide (CaO, main reflexes at 2.41, 2.78 Å, etc.). In addition, 50.3 wt% calcium carbonate remains in the sample (Table 2, Figure 2b).

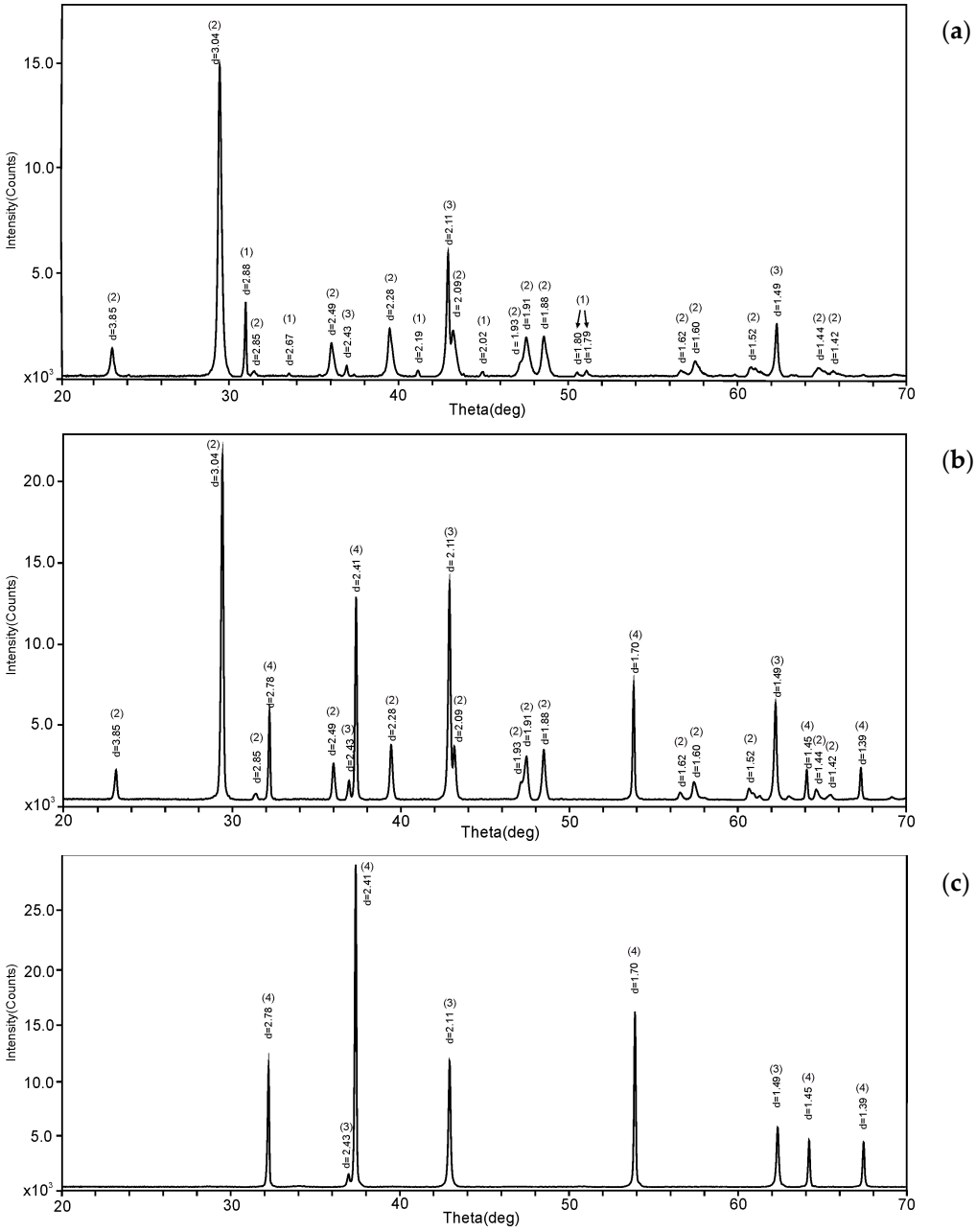


**Figure 2.** X-ray diffraction patterns of dolomite samples: initial (**a**) and calcined at 720 °C (**b**) and 750 °C (**c**), (1)—$CaMg(CO_3)_2$ (Dolomite); (2)—$CaCO_3$ (Calcite), (3)—MgO (Periclase); (4)—CaO (Calcium Oxide).

**Table 2.** Composition of dolomite samples calcined at 720 and 750 °C (calculation by Rietveld method).

| Phase | Component Phase (wt%) | |
|---|---|---|
| | **720 °C** | **750 °C** |
| $CaCO_3$ | 50.3 | - |
| MgO | 34.9 | 45.9 |
| CaO | 14.8 | 54.1 |

It was noted that after calcination of the dolomite sample at 750 °C (Figure 2c), both magnesium carbonate and calcium carbonate decomposed to magnesium and calcium oxides, respectively. The sample was found to contain 54.1 wt% calcium oxide and 45.9 wt% magnesium oxide (Table 2).

When studying the morphology of the particles of the initial dolomite powder, it was shown that it consists of particles of flake shape with a size mainly up to 1 µm (Figure 3a). It was noted that, as a result of calcination, the particles are partially sintered (Figure 3b,c). For example, after calcination at 750 °C, dolomite particles with a shape close to a hexagonal crystal and about 2 µm in size were found covered with smaller particles (Figure 3c). The results of SEM/EDS analysis are shown in Figure S1 and Table S1 (see Supplementary Materials). The example of a sample of dolomite calcined at 750 °C shows the distribution maps of elements (see Supplementary Materials, Figure S2).

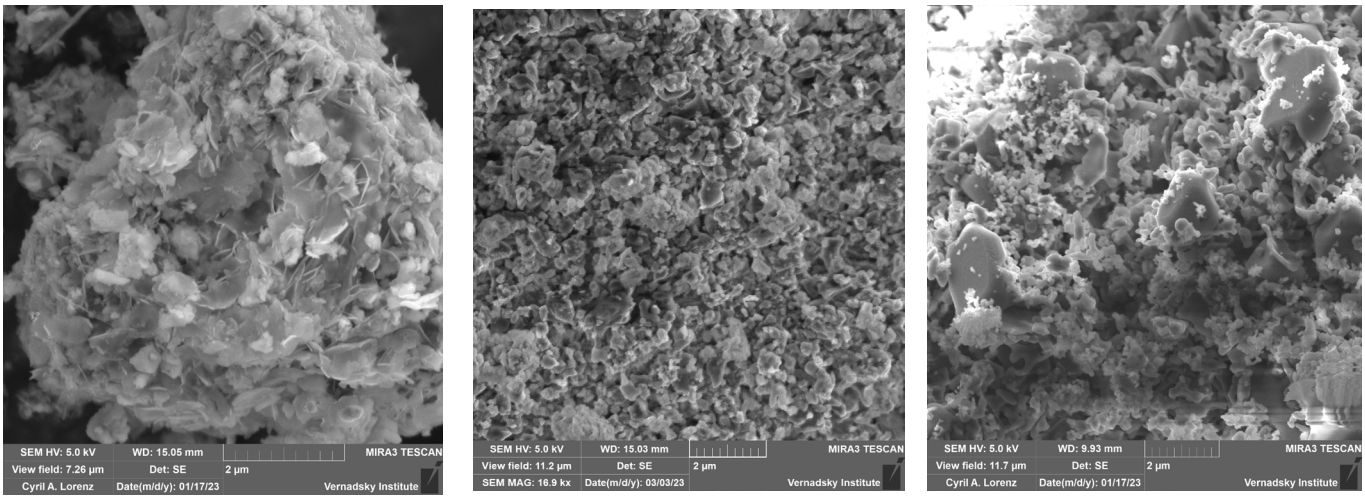


(**a**) (**b**) (**c**)

**Figure 3.** Scanning electron microscope (SEM) images of dolomite samples: initial (**a**), calcined at 720 °C (**b**), and calcined at 750 °C (**c**).

### *3.2. Study of the MPP Matrix Samples*

Calcined dolomite powders, the characteristics of which are given in Section 3.1, were used for the synthesis of the MPP matrix. From the results of XRD and XRF, it was found that samples of dolomite powder calcined at 720 and 750 °C contain 34.9 and 45.9 wt% MgO, respectively. MPP matrix samples were synthesized using calcined powders with the above-mentioned MgO content as well as an excess of MgO in relation to the stoichiometry of reaction (1) was 10 wt%, as previously shown in [34]. Component weight ratios were as follows: calcined at 720 or 750 °C, dolomite powder:$H_2O$:$KH_2PO_4$ ratio of (2.87 or 2.18, respectively):2:3.

The X-ray diffraction patterns of the obtained MPP matrix samples are shown in Figure 4. Crystalline phases of the target matrix composition $MgKPO_4 \times 6H_2O$ (struvite-(K), main reflexes at 4.25; 2.90; 4.13 Å, etc.) as well as MgO (periclase, main reflexes at 2.11, 1.49 Å, etc.), previously taken in excess, were found in all the studied samples.

It was found that the sample MPP_dolomite_720 (Figure 4a) retained the phase of calcite ($CaCO_3$), which was present in the dolomite sample calcined at 720 °C (Figure 2b).

The calcium hydroxide phase ($Ca(OH)_2$, main reflexes at 2.63, 4.92 Å, etc.) was shown to be present in the MPP_dolomite_750 sample (Figure 4b), which is formed by the interaction of calcium oxide with water [35]. Since calcium oxide is very corrosive and reacts violently with water, $Ca(OH)_2$ can also be formed by the reaction of CaO with $H_2O$ from air during storage, as previously shown in [28]. However, all phases found in the sample have low solubility in water; for example, the solubility product ($K_{sp}$) at 25 °C of $CaCO_3$ is 3.3–$10^{-9}$ [36] and $Ca(OH)_2$ is 5.02–$10^{-6}$ [37]).

The SEM micrographs of the sample surface of the MPP matrix are shown in Figures 5 and 6. It was found that the sample MPP_dolomite_720 has a pore size of 100–200 µm (Figure 5a) and is composed mainly of columnar crystals (Figure 5b). In the sample, particles with a size of 2–3 microns were also found (Figure 5b); apparently, it is a phase of calcium carbonate

detected by the XRD method (Figure 2b). It was noted that the sample MPP_dolomite_750 has macropores ranging in size from 140 to 500 µm (Figure 6a) and micropores up to 10 µm (Figure 6b).

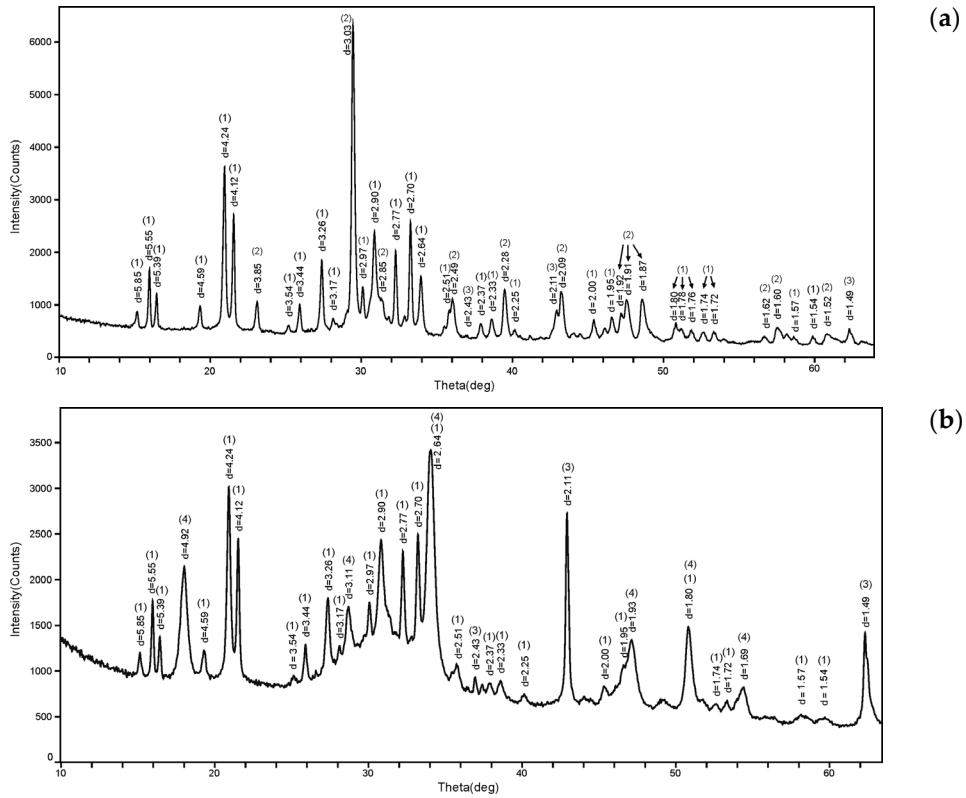


**Figure 4.** X-ray diffraction patterns of the magnesium potassium phosphate (MPP) matrix: MPP_dolomite_720 (**a**) and MPP_dolomite_750 (**b**), (1)—$MgKPO_4 \times 6H_2O$ (Struvite-(K)); (2)—$CaCO_3$ (Calcite); (3)—MgO (Periclase); (4)—$Ca(OH)_2$ (Calcium Hydroxide).

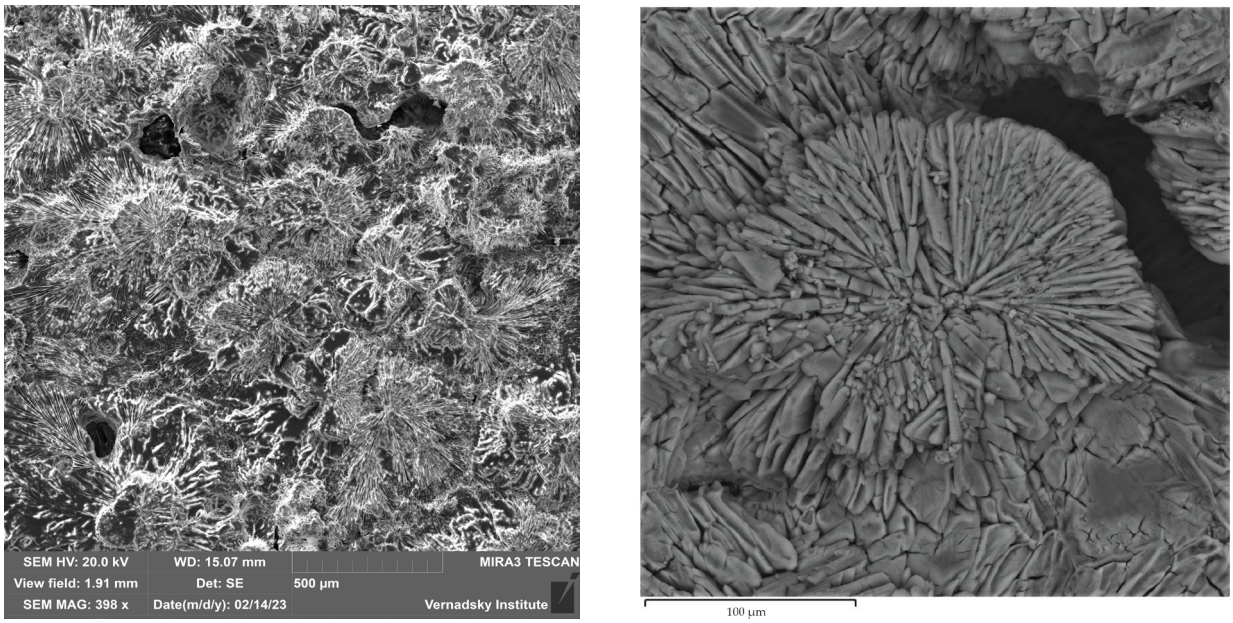


(**a**) (**b**)

**Figure 5.** SEM images of the MPP_dolomite_720 sample in (**a**) secondary electrons (SE) and (**b**) back-scattering electrons (BSE).

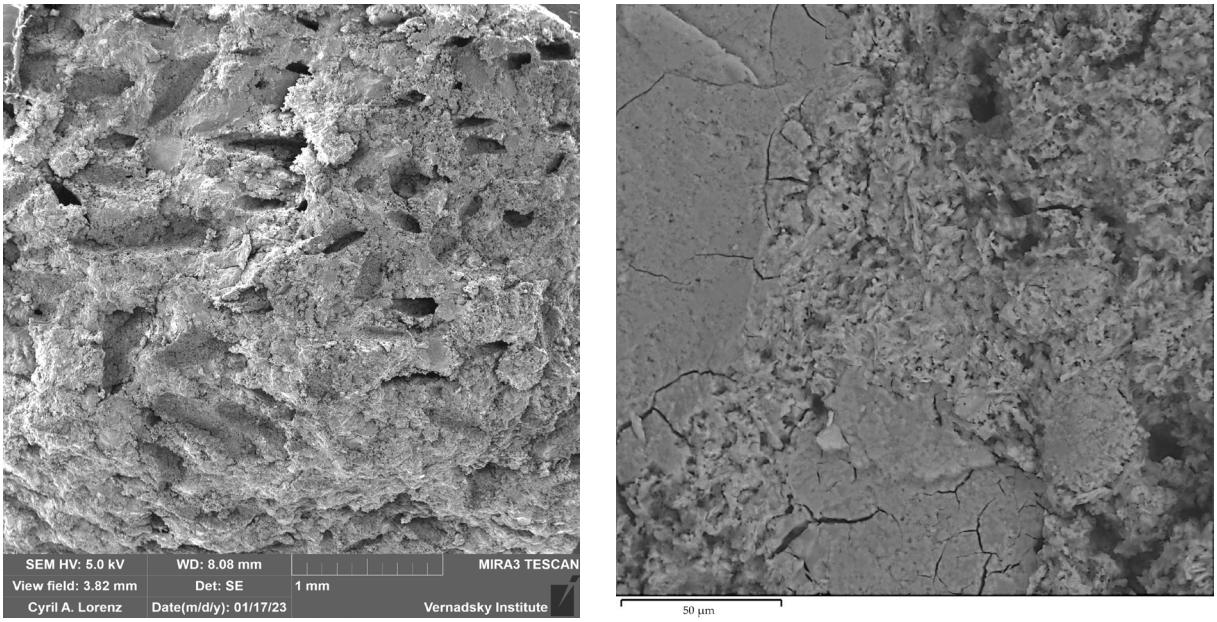


(**a**) (**b**)

**Figure 6.** SEM images of the MPP_dolomite_750 sample in (**a**) secondary electrons (SE) and (**b**) backscattering electrons (BSE).

The densities of samples MPP_dolomite_720 and MPP_dolomite_750 were 1.88 and 1.67 g/cm$^3$, respectively (Table 3). It was found that the volumetric porosity (PV) and apparent porosity (PA) of the MPP_dolomite_720 sample are 4 and 2 times lower, respectively, than these values of the MPP_dolomite_750 sample (Table 3). At the same time, the obtained PA values for the MPP matrix of about 9.3% are significantly lower than the PA values of magnesium ammonium phosphate matrix samples of composition $MgNH_4PO_4 \times 6H_2O$ prepared using dolomite calcined at 720 °C and containing $CaCO_3$, which were 45% [28].

**Table 3.** Properties of MPP matrix samples obtained using dolomite.

| Parameter | Sample | |
|---|---|---|
| | MPP_dolomite_720 | MPP_dolomite_750 |
| Density (ρ), g/cm$^3$ | 1.88 | 1.67 |
| Volumetric porosity (PV), % | 2.1 | 8.3 |
| Apparent porosity (PA), % | 9.3 | 19.0 |
| Compressive strength, MPa | 25.8 | 7.5 |

The compressive strengths of MPP_dolomite_720 and MPP_dolomite_750 samples were about 25.8 and 7.5 MPa, respectively (Table 3). Earlier, it was shown that the strength of the MPP matrix obtained using only MgO after 1300 °C calcination is about 6.2 MPa [22]. All of the indicated values are in accordance with the regulatory requirements for a cement compound (no less than 4.9 MPa) [38]. Thus, the calcium carbonate present in the MPP_dolomite_720 sample plays the role of a reinforcing agent for the matrix, which leads to an increase in compressive strength, as we noted earlier [31]. On the other hand, the absence of this phase and the presence of the calcium hydroxide phase lead to a significant decrease in the strength of MPP_dolomite_750 samples.

For the study of hydrolytic stability, the sample MPP_dolomite_720 was chosen, which has higher quality indicators to solve the problem of RW conditioning.

The hydrolytic stability data of the MPP_dolomite_720 sample and the blank MPP matrix obtained using commercial MgO calcined at 1300 °C [34] were compared. It was shown that the leaching rates of structure-forming elements from MPP_dolomite_720 and from the MPP matrix are similar (Figure 7). The differential leaching rates of potassium,

phosphorus, magnesium, and calcium from the MPP_dolomite_720 sample (Figure 7) are: $2.2 \times 10^{-4}$, $6.6 \times 10^{-5}$, $4.6 \times 10^{-5}$, and $2.5 \times 10^{-6}$ g/(cm$^2$·day), respectively.

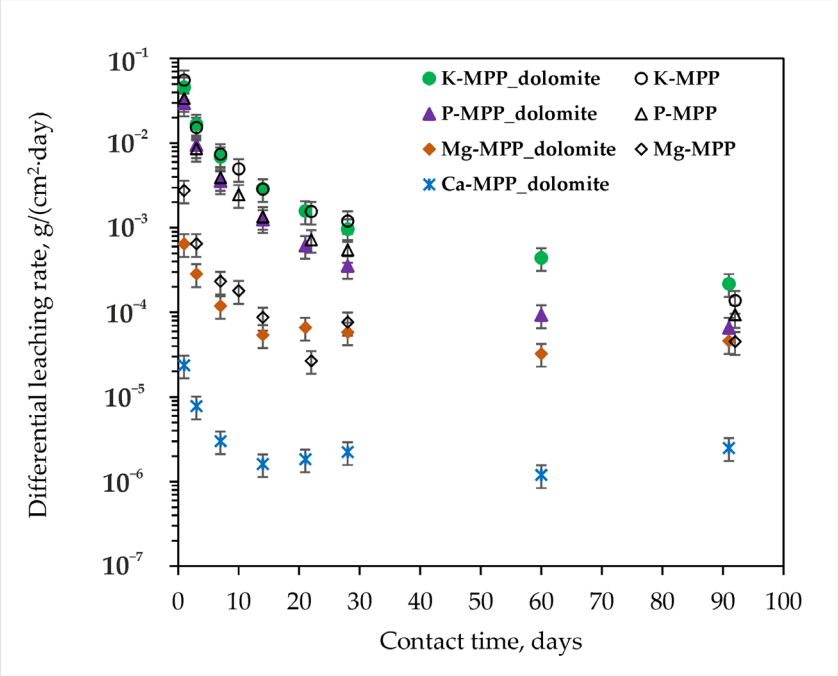


**Figure 7.** Kinetic curve of the leaching rate of the matrix components from the MPP matrix samples.

A high hydrolytic resistance of the MPP compound to leaching of simulants of RW components was established (Figure 8). The differential leaching rate of cesium from MPP_dolomite_720 samples on the 28th day of contact of samples with water was $3.7 \times 10^{-5}$ g/(cm$^2$·day), which corresponds to the normative requirements for ILW: no more than $10^{-3}$ g/(cm$^2$·day) for $^{137}$Cs [38].

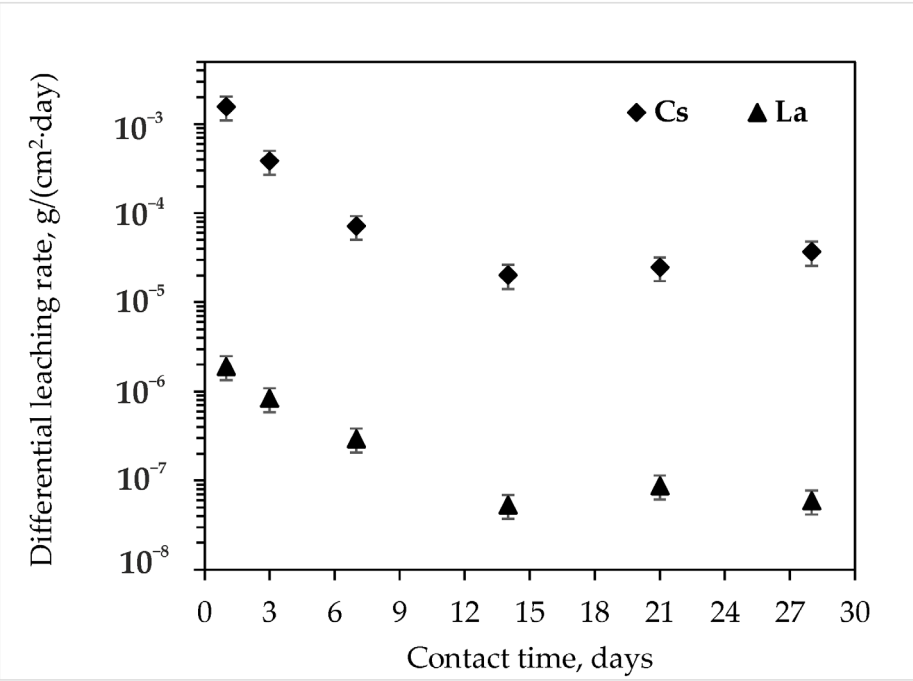


**Figure 8.** Kinetic curve of the leaching rate of the Cs and La from the MPP_dolomite_720 samples.

It was found that the differential leaching rate of lanthanum from MPP_dolomite_720 samples on the 28th day of contact of samples with water was extremely low—$5.9 \times 10^{-8}$ g/(cm$^2$·day). This value is lower than the lanthanum leaching rate of $4.1 \times 10^{-6}$ g/(cm$^2$·day) from MPP matrix containing 6.7 wt% and obtained using MgO calcined at 1300 °C [39] and corresponds to the known data on rare earth elements (REE) leaching from high temperature matrix-borosilicate glass (REE leaching rate is ~$10^{-8}$ g/(cm$^2$·day)) [40].

## 4. Conclusions

In this study, a new synthesis method of MPP matrix using a magnesium source is proposed using the example of a sample of dolomite raw material of the composition $MgCa(CO_3)_2$, $CaCO_3$, and MgO. The following main conclusions can be drawn:

- Calcination of dolomite at 720 °C for 1.5 h results in the production of MgO, CaO, and $CaCO_3$ in the ratios of 1.00, 0.42, and 1.44, respectively. Increasing the calcination temperature of dolomite up to 750 °C and the calcination time up to 24 h results in the decomposition of $CaCO_3$ and the production of CaO; the resulting MgO/CaO ratio was 1/1.18.
- The target crystalline phase of the matrix, $MgKPO_4 \times 6H_2O$, was confirmed in all the studied MPP compounds obtained from calcined dolomite samples. At the same time, differences in calcination conditions resulted in compounds with different properties. It was shown that the quality indicators of compound obtained from dolomite after calcination at 720 °C exceed those of compound obtained from dolomite after calcination at 750 °C to solve the problem of RW conditioning. Thus, the compound under milder calcination conditions (720 °C, 1.5 h) has a higher density (1.88 g/cm$^3$ vs. 1.67 g/cm$^3$) and strength (25.8 MPa vs. 7.5 MPa) with reduced porosity (PV and PA are 4 and 2 times less, respectively).
- It should be especially emphasized that the leaching rate of structure-forming elements from the MPP compound obtained from dolomite after calcination at 720 °C is similar to their leaching rate from the blank MPP matrix obtained by using expensive magnesium oxide as a hardener. Thus, the differential leaching rates of K, P, and M from the compound are $2.2 \times 10^{-4}$, $6.6 \times 10^{-5}$, $4.6 \times 10^{-5}$ g/(cm$^2$·day), respectively. Most importantly, the leaching rates of RW components from this compound meet the normative requirements for industrial cement matrices. The differential leaching rate of cesium from the compound was $3.7 \times 10^{-5}$ g/(cm$^2$·day), which corresponds to the normative requirements in Russia: no more than $10^{-3}$ g/(cm$^2$·day).

Thus, the key problem of the nuclear power industry—reliable RW immobilization—can be solved by using a compound obtained from the widely available and low-cost natural mineral raw material dolomite.

**Supplementary Materials:** The following supporting information can be downloaded at: https://www.mdpi.com/article/10.3390/en16145513/s1, Figure S1: Scanning electron microscope (SEM) images of dolomite samples in backscattered electrons: initial (a), calcined at 720 °C (b), and calcined at 750 °C (c); Table S1: Average data of elemental composition (at%) of dolomite powder samples according to EDS date; Figure S2: SEM image (a) and multilayer image (b) of the dolomite sample calcined at 750 °C with elemental distribution maps of magnesium (c) and calcium (d) in sample.

**Author Contributions:** Conceptualization, S.A.K. and K.Y.B.; methodology, S.A.K. and S.E.V.; validation, S.A.K., K.Y.B., A.V.F. and S.E.V.; formal analysis, S.A.K.; K.Y.B. and A.V.F.; investigation, A.V.F. and K.Y.B.; resources, S.E.V.; writing—original draft preparation, S.A.K.; writing—review and editing, S.E.V.; visualization, S.A.K. and S.E.V.; supervision, S.E.V.; project administration, S.A.K.; funding acquisition, S.A.K. All authors have read and agreed to the published version of the manuscript.

**Funding:** This research was funded by the Russian Science Foundation grant number 22-73-10202, https://rscf.ru/en/project/22-73-10202/.

**Data Availability Statement:** Not applicable.

**Acknowledgments:** The authors thank I.N. Gromyak, A.V. Zhilkina and T.G. Kuzmina (Laboratory of Methods for Investigation and Analysis of Substances and Materials, GEOKHI RAS) for carrying out ICP-AES, ICP-MS and XRF analyses, as well as to K.A. Lorenz and S.N. Teplyakova (Meteoritics laboratory, GEOKHI RAS) for the analysis of the samples by the SEM/EDS method.

**Conflicts of Interest:** The authors declare no conflict of interest. The funders had no role in the design of the study; in the collection, analyses, or interpretation of data; in the writing of the manuscript; or in the decision to publish the results.

## References

1. International Atomic Energy Agency. Available online: https://www.iaea.org/topics/radioactive-waste-and-spent-fuel-management (accessed on 28 April 2023).
2. Ojovan, M.I.; Steinmetz, H.J. Approaches to Disposal of Nuclear Waste. *Energies* **2022**, *15*, 7804. [CrossRef]
3. Drace, Z.; Ojovan, M.I.; Samanta, S.K. Challenges in Planning of Integrated Nuclear Waste Management. *Sustainability* **2022**, *14*, 14204. [CrossRef]
4. Kulikova, S.A.; Danilov, S.S.; Matveenko, A.V.; Frolova, A.V.; Belova, K.Y.; Petrov, V.G.; Vinokurov, S.E.; Myasoedov, B.F. Perspective Compounds for Immobilization of Spent Electrolyte from Pyrochemical Processing of Spent Nuclear Fuel. *Appl. Sci.* **2021**, *11*, 11180. [CrossRef]
5. Corkhill, C.; Hyatt, N. *Nuclear Waste Management*; IOP Publishing Ltd.: Bristol, UK, 2018; pp. 1–30.
6. Rakhimova, N. Recent Advances in Alternative Cementitious Materials for Nuclear Waste Immobilization: A Review. *Sustainability* **2023**, *15*, 689. [CrossRef]
7. Covill, A.; Hyatt, N.C.; Hill, J.; Collier, N.C. Development of magnesium phosphate cements for encapsulation of radioactive waste. *Adv. Appl. Ceram.* **2011**, *110*, 151–156. [CrossRef]
8. Cau Dit Coumes, C.; Lambertin, D.; Lahalle, H.; Antonucci, P.; Cannes, C.; Delpech, S. Selection of a mineral binder with potentialities for the stabilization/solidification of aluminum metal. *J. Nucl. Mater.* **2014**, *453*, 31–40. [CrossRef]
9. Gardner, L.J.; Walling, S.A.; Lawson, S.M.; Sun, S.; Bernal, S.A.; Corkhill, C.L.; Provis, J.L.; Apperley, D.C.; Iuga, D.; Hanna, J.V.; et al. Characterization of and Structural Insight into Struvite-K, $MgKPO_4{\cdot}6H_2O$, an Analogue of Struvite. *Inorg. Chem.* **2021**, *60*, 195–205. [CrossRef] [PubMed]
10. Holdsworth, A.F.; Eccles, H.; Halman, A.M.; Mao, R.; Bond, G. Low-Temperature Continuous Flow Synthesis of Metal Ammonium Phosphates. *Sci. Rep.* **2018**, *8*, 13547. [CrossRef]
11. Wagh, A.S. *Chemically Bonded Phosphate Ceramics: Twenty-First Century Materials with Diverse Applications*, 2nd ed.; Elsevier: Amsterdam, The Netherlands, 2016; pp. 1–422; ISBN 978-0-08-100380-0.
12. Vinokurov, S.E.; Kulikova, S.A.; Frolova, A.V.; Danilov, S.S.; Belova, K.Y.; Rodionova, A.A.; Myasoedov, B.F. New Methods and Materials in Nuclear Fuel Fabrication and Spent Nuclear Fuel and Radioactive Waste Management. In *Advances in Geochemistry, Analytical Chemistry, and Planetary Sciences*; Kolotov, V.P., Bezaeva, N.S., Eds.; Springer: Cham, Switzerland, 2023; pp. 579–594. [CrossRef]
13. Kulikova, S.A.; Belova, K.Y.; Tyupina, E.A.; Vinokurov, S.E. Conditioning of Spent Electrolyte Surrogate LiCl-KCl-CsCl Using Magnesium Potassium Phosphate Compound. *Energies* **2020**, *13*, 1963. [CrossRef]
14. Graeser, S.; Postl, W.; Bojar, H.-P.; Berlepsch, P.; Armbruster, T.; Raber, T.; Ettinger, K.; Walter, F. Struvite-(K), $KMgPO_4{\cdot}6H_2O$, the potassium equivalent of struvite—A new mineral. *Eur. J. Miner.* **2008**, *20*, 629–633. [CrossRef]
15. Milestone, N.B. Reactions in cement encapsulated nuclear wastes: Need for toolbox of different cement types. *Adv. Appl. Ceram.* **2006**, *105*, 13–20. [CrossRef]
16. Wagh, A.S.; Strain, R.; Jeong, S.Y.; Reed, D.; Krause, T.; Singh, D. Stabilization of Rocky Flats Pu-contaminated ash within chemically bonded phosphate ceramics. *J. Nucl. Mater.* **1999**, *265*, 295–307. [CrossRef]
17. Lai, Z.; Lai, X.; Shi, J.; Lu, Z. Effect of $Zn^{2+}$ on the early hydration behavior of potassium phosphate based magnesium phosphate cement. *Constr. Build. Mater.* **2016**, *129*, 70–78. [CrossRef]
18. Banks, E.; Chianelli, R.; Korenstein, R. Crystal Chemistry of Struvite Analogs of the Type $MgMPO_4{\cdot}6H_2O$ (M+ = $K^+$, $Rb^+$, $Cs^+$, $T1^+$, $NH^{4+}$). *Inorg. Chem.* **1975**, *14*, 1634–1639. [CrossRef]
19. Wagh, A.; Sayenko, S.; Shkuropatenko, V.; Tarasov, R.; Dykiy, M.P.; Svitlychniy, Y.O.; Virych, V.; Ulybkina, E.A. Experimental study on cesium immobilization in struvite structures. *J. Hazard. Mater.* **2016**, *302*, 241–249. [CrossRef] [PubMed]
20. Walling, S.A.; Provis, J.L. Magnesia-based cements: A journey of 150 years, and cements for the future? *Chem. Rev.* **2016**, *116*, 4170–4204. [CrossRef]
21. Chartier, D.; Sanchez-Canet, J.; Antonucci, P.; Esnouf, S.; Renault, J.-P.; Farcy, O.; Lambertin, D.; Parraud, S.; Lamotte, H.; Cau Dit Coumes, C. Behaviour of magnesium phosphate cement-based materials under gamma and alpha irradiation. *J. Nucl. Mater.* **2020**, *541*, 152411. [CrossRef]
22. Vinokurov, S.E.; Kulikova, S.A.; Krupskaya, V.V.; Tyupina, E.A. Effect of characteristics of magnesium oxide powder on composition and strength of magnesium potassium phosphate compound for solidifying radioactive waste. *Russ. J. Appl. Chem.* **2019**, *92*, 490–497. [CrossRef]

23. Formosa, J.; Lacasta, A.M.; Navarro, A.; del Valle-Zermeño, R.; Niubó, M.; Rosell, J.R.; Chimenos, J.M. Magnesium Phosphate Cements formulated with a low-grade MgO by-product: Physico-mechanical and durability aspects. *Constr. Build. Mater.* **2015**, *91*, 150–157. [CrossRef]
24. Kulikova, S.A.; Vinokurov, S.E.; Khamizov, R.K.; Vlasovskikh, N.S.; Belova, K.Y.; Dzhenloda, R.K.; Konov, M.A.; Myasoedov, B.F. The Use of MgO Obtained from Serpentinite in the Synthesis of a Magnesium Potassium Phosphate Matrix for Radioactive Waste Immobilization. *Appl. Sci.* **2021**, *11*, 220. [CrossRef]
25. Yu, J.; Qian, J.; Wang, F.; Li, Z.; Jia, X. Preparation and properties of a magnesium phosphate cement with dolomite. *Cem. Concr. Res.* **2020**, *138*, 106235. [CrossRef]
26. Yang, Q.; Zhang, S.; Wu, X. Deicer-scaling resistance of phosphate cement-based binder for rapid repair of concrete. *Cem. Concr. Res.* **2002**, *32*, 165–168. [CrossRef]
27. Yu, J.; Qian, J.; Wang, F.; Qin, J.; Dai, X.; You, C.; Jia, X. Study of using dolomite ores as raw materials to produce magnesium phosphate cement. *Constr. Build. Mater.* **2020**, *253*, 119147. [CrossRef]
28. Baghriche, M.; Achour, S.; Baghriche, O. Combined effect of cement kiln dust and calcined dolomite raw on the properties of performance magnesium phosphate cement. *Case Stud. Constr. Mater.* **2020**, *13*, e00386. [CrossRef]
29. Kristóf-Makó, É.; Juhász, A.Z. The effect of mechanical treatment on the crystal structure and thermal decomposition of dolomite. *Thermochim. Acta* **1999**, *342*, 105–114. [CrossRef]
30. Abdullah, S.F.A.; Saleh, S.S.M.; Mohammad, N.F.; Idris, M.S.; Saliu, H.R. Effect of Thermal Treatment on Natural Dolomite. *J. Phys. Conf. Ser.* **2021**, *2080*, 012009. [CrossRef]
31. Dmitrieva, A.V.; Kalenova, M.Y.; Kulikova, S.A.; Kuznetsov, I.V.; Koshcheev, A.M.; Vinokurov, S.E. Magnesium-Potassium Phosphate Matrix for Immobilization of $^{14}$C. *Russ. J. Appl. Chem.* **2018**, *91*, 641–646. [CrossRef]
32. *GOST R 52126-2003*; Radioactive Waste. Long Time Leach Testing of Solidified Radioactive Waste Forms. Gosstandart 305: Moscow, Russia, 2003; pp. 1–8.
33. Mandrino, D.; Paulin, I.; Kržmanc, M.M.; Škapin, S.D. Physical and chemical treatments influence on the thermal decomposition of a dolomite used as a foaming agent. *J. Therm. Anal. Calorim.* **2018**, *31*, 1125–1134. [CrossRef]
34. Vinokurov, S.E.; Kulikova, S.A.; Krupskaya, V.V.; Myasoedov, B.F. Magnesium potassium phosphate compound for radioactive waste immobilization: Phase composition, structure, and physicochemical and hydrolytic durability. *Radiochemistry* **2018**, *60*, 70–78. [CrossRef]
35. Ropp, R.C. Group 16 (O, S, Se, Te) Alkaline Earth Compounds. In *Encyclopedia of the Alkaline Earth Compounds*; Elsevier: Oxford, UK, 2013; Chapter 3; pp. 105–197. [CrossRef]
36. Benjamin, M.M. *Water Chemistry*, 2nd ed.; McGraw-Hill: New York, NY, USA, 2002; ISBN 978-0-07-238390-4.
37. Rumble, J.R. *Handbook of Chemistry and Physics*, 99th ed.; CRC Press: Boca Raton, FL, USA, 2018; ISBN 978-1138561632.
38. *NP-019-15*; Federal Norms and Rules in the Field of Atomic Energy Use "Collection, Processing, Storage and Conditioning of Liquid Radioactive Waste. Safety Requirements"; With Changes (Order No. 299 Dated 13 September 2021). Rostekhnadzor: Moscow, Russia, 2015; pp. 1–22.
39. Vinokurov, S.E.; Kulikova, S.A.; Myasoedov, B.F. Magnesium Potassium Phosphate Compound for Immobilization of Radioactive Waste Containing Actinide and Rare Earth Elements. *Materials* **2018**, *11*, 976. [CrossRef]
40. Ojovan, M.I.; Lee, W.E. Glassy Wasteforms for Nuclear Waste Immobilization. *Metall. Mater. Trans. A* **2011**, *42A*, 837–851. [CrossRef]